

On the Rheological Behavior of Frozen Soil (Part II)

By Yoshiaki FUKUO

(Manuscript received June 30, 1966)

Abstract

In order to examine the rheological behavior of frozen soil, an experiment of flexure was carried out, using the samples moulded into beam with 4 cm square cross-section and 50 cm span length. The equation which represented the deflection of frozen soil beam, was derived from certain assumptions usually accepted in elastic bending, on the basis of the Murayama-Shibata theory for the rheological characters of unfrozen clay.

The result of the experiment was analysed by this equation and the important creep factors σ_0 and B_2E_2 in their theory were evaluated for frozen soil. These values of factors were compared with those calculated from the experiment of axial compression of the same frozen soil, as already reported in Part I. Comparison showed fairly close agreement.

1. Introduction

It is well known that the freezing of water in soil causes various interesting phenomena such as the heaving of soil¹⁾, the remaining of unfrozen water²⁾, which is closely related to the adhesion and adsorption on the interface between the soil particle and water^{3,4)}, and plays an important role in the development of nival geomorphologic features⁵⁾ through the processes of particle sorting, stone migration and rock weathering⁶⁾. Recently in our country, the freezing method of soil in engineering construction has been in progress⁷⁾. The strength of freezing soil is perhaps dependent on the cohesion between the ice and particles and on unfrozen water⁸⁾. For the safety of construction, the strength of frozen soil and the behavior of heaving must be understood exactly and fully.

So an experiment of compression in axial direction was carried out, using the frozen soil moulded in cylindrical form of 5 cm in diam. and 9 cm in height, and its result was reported in Part I⁹⁾. Concurrently, an experiment of flexure of frozen soil was carried out for the beam with 4 cm sq. in cross-section and 50 cm length in span. The results of this examination will be reported here.

2. Soil samples

In May 1965, earth soil was frozen near Kanasugi Bridge in Tokyo for the preexamination of the freezing method of construction, and a vertical pit with diam. 2 m was bored there from the surface to a depth 10 m. On the sidewall of this pit, the blocks of frozen soil were sampled at 5, 7, 8.5 and 10 m depth: two blocks to each depth, one for undisturbed soil and the other for remoulded soil. All blocks were packed dubly with vinyl sacks to prevent the evaporation of water in soil.

As undisturbed blocks were not large enough to be trimmed into the beam with 4cm sq. in cross-section and 50cm in span, all test pieces were made from remoulded blocks. Blocks were melted and stuffed into the moulding case for the beam and frozen again for two days in a brine box kept at a temperature of $-23^{\circ}\text{C}\pm 1^{\circ}\text{C}$. Soon after being moulded, these pieces were coated all over their surface with vinyl sheets of 0.1mm thickness to prevent the evaporation of water in pieces and put on a bending device, as seen in the next paragraph.

Blocks at 5, 7 and 8.5m depth were silty clay appreciably consolidated. Blocks at 10m depth were silty sand containing gravel and fragments of shell. The properties of this clay and sand are shown in Tables 1 and 2.

TABLE 1.

Consistency limits and water contents of silty clay scrapped from undisturbed frozen blocks sampled at 5, 7 and 8.5 m depth layers.

depth (m)	5	7	8.5
plastic limit (%)	37.0	37.6	35.4
liquid limit (%)	71.0	70.2	70.7
water content (%)	51.0	52.7	46.4

TABLE 2.

Grain size distribution and water content of silty sand scrapped from undisturbed frozen block sampled at 10 m depth layer.

	total sieving weight in dry	390.9 gr							
	water content	25.0 %							
mesh size (μ)	>2380	2380>							
weight (gr)	234.2	155.8							
	sieving loss	0.9 gr							
Grain size distribution less than 2380 μ mesh									
mesh size (μ)	>2000	>1410	>1000	>710	>500	>350	>250	>210	210>
weight percentage	11.4	18.6	1.55	14.0	11.0	17.4	5.6	1.6	4.9

3. Instrument and method of experiment

The schema of bending device is shown in Fig. 1. A test piece was set on the supports (A) and (B). The distance (span) between them was 50 cm. The center load (P) was put on the central cross section of beam span and a test piece was bent vertically downward. The supports (A) and (B) were made from the steel bar with semicircular cross-section of 2cm diam. to prevent sharp edge cutting. The deflection of beam was measured at each quarter point (a) (center), (b) and (c) by linear differential transformers, and detected on the dotting auto-recorder with accuracy of $\pm 0.04\text{mm}$.

The bending device was placed in freezing box which had a net capacity of

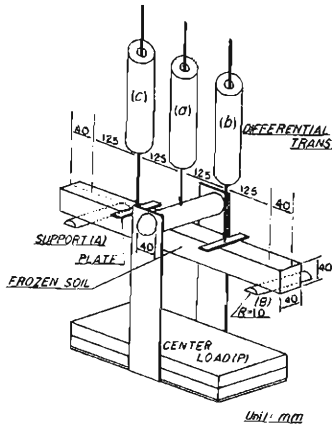


Fig. 1. The schema of flexure device.

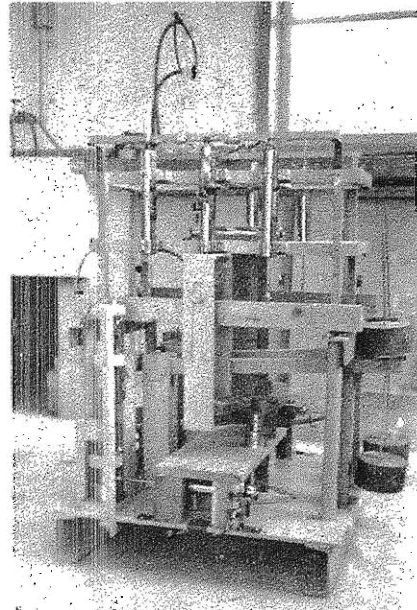


Photo. 1. The view of flexure device.

0.7m in width, 0.8m in depth and 0.9m in height, and was cooled by an electric refrigerator. The temperature in the freezing box was controlled at a constant temperature by a thermostat and stirring fan with accuracy of $\pm 0.5^{\circ}\text{C}$. Photo. 1 shows the view of the bending device.

Loading and unloading of weights forced the opening of the door of the freezing box for about two minutes and consequently disturbed the constancy of temperature by the inflow of outer air. So dotted records for about five minutes after loading and unloading did not show the deformation of the test piece at constant temperature and weights.

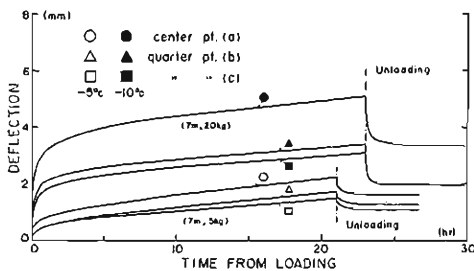


Fig. 2. Typical examples of deflections and recoveries of frozen soil beams.

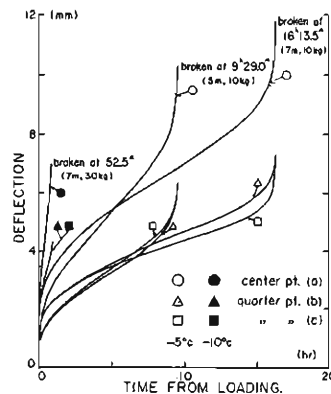


Fig. 3. Typical examples of deflections of beams broken at about central cross-section.

4. Analytical method

The typical results of experiments of bending deflection are shown in Figs. 2 and 3. The beams were bent by constant center load and recovered after unloading, or were broken at about the central cross-section of span. In these figures, it is seen apparently that the flexure of beams was not elastic but creeping deformation.

As reported in Part I, the deformation of frozen soil in axial compression has been analysed according to the theory of Drs. Murayama and Shibata¹⁰⁾ for the creeping deformation of unfrozen clay, and valuable results have been obtained. Hence it is intended that the deflection of frozen soil beam should also be analysed with reference to their theory.

The obtained deflection is small compared with the thickness, width and, of course, span length as seen in Fig. 2. Then, as usually treated with the elastic bending, the analysis of flexure of frozen soil may be analysed on the basis of the following assumptions:—

- i) The beam is of homogeneous frozen soil which has the same rheological characters in tension and compression.
- ii) The beam has a neutral surface on which the longitudinal displacement of material point is negligible.
- iii) Plane section of the beam always remains plane and the strain is proportional to the distance from the neutral surface.

After the constant load P is applied to the central section of the beam span, the compressive and tensile stresses are exerted at any material point above and below the neutral surface respectively, and the strains are increased rheologically, satisfying the assumptions as stated above. According to the theory of Drs. Murayama and Shibata, the strain ϵ is given by

$$\epsilon = \frac{\sigma}{E_1} + \frac{\sigma - \sigma_0}{E_2} - \frac{2(\sigma - \sigma_0)}{B_2 E_2} \tanh^{-1} \left\{ \exp(-A_2 B_2 E_2 t) \tanh \frac{B_2}{2} \right\}$$

under constant stress σ smaller than the upper yield value σ_v ,

where, E_1 : Young's modulus between the matrixes of particles

E_2 : Young's modulus in a matrix

σ_0 : lower yield value of clay

t : time measured from loading

A_2 and B_2 : proper constants of clay depending on temperature

Fig. 4 represents a beam under load and shows the coordinating system and various dimensions and notations that appear in the equations, as will be seen later.

If the center load P is adequately small, the bending stress at any point does not exceed the lower yield value σ_0 and the beam will be deflected elastically, but if the load P is large, the bending stress reaches the value of σ_0 at certain levels $z = h'$, and above and below these levels the strain will be increased with time even under constant load.

In the interval $|z| \leq h'$, the deformation is elastic and the strain ϵ_z at $z = z$ is given by

$$\frac{z}{h'} = \frac{\epsilon_z}{\epsilon_{h'}} = \frac{\sigma_z}{\sigma_{h'}} \quad (1)$$

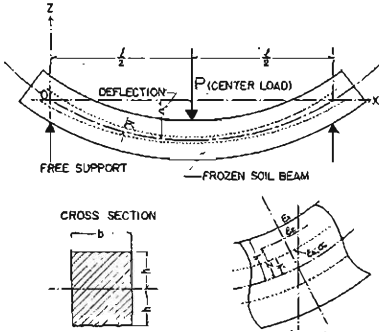


Fig. 4. Coordinating system and various dimensions and notations for the deflection.

where, σ_z , $\sigma_{h'}$ and ε_z , $\varepsilon_{h'}$ are the stresses and strains at the levels $z=z$ and h' .

As the value of $\sigma_{h'}$ is equal to the lower yield value σ_0 ,

$$\sigma_z = \sigma_0 \frac{z}{h'} \quad \text{for } |z| \leq h' \quad (2)$$

In the interval $h' < |z| \leq h$, the bending strain ε_z is given by

$$\varepsilon_z = \frac{\sigma_z}{E_1} + \frac{\sigma_z - \sigma_0}{E_2} - \frac{2(\sigma_z - \sigma_0)}{B_2 E_2} \times \tanh^{-1} \left\{ \exp(-A_2 B_2 E_2 t) \tanh \frac{B_2}{2} \right\} \quad (3)$$

Noting that,

$$\frac{1}{F_2(t)} \equiv \frac{1}{E_2} - \frac{2}{B_2 E_2} \tanh^{-1} \left\{ \exp(-A_2 B_2 E_2 t) \tanh \frac{B_2}{2} \right\} \quad (4)$$

then eq. (3) is rewritten as

$$\varepsilon_z = \left(\frac{1}{E_1} + \frac{1}{F_2} \right) \sigma_z - \frac{1}{F_2} \sigma_0 \quad (5)$$

From the assumption (iii),

$$\frac{z}{h'} = \frac{\varepsilon_z}{\varepsilon_{h'}} = \frac{E_1}{\sigma_0} \varepsilon_z \quad (6)$$

and from eqs. (5) and (6),

$$\sigma_z = \frac{\sigma_0}{E_1 + F_2} \left(E_1 + F_2 \frac{z}{h'} \right) \quad \text{for } h' < |z| \leq h \quad (7)$$

If the beam is bent slightly and the deflection is considered to be increased quasistatically, that is, the moment M due to the center load P is balanced to the moment exerted by the bending stress σ_z at any time,

$$\begin{aligned} M &= \int_{-h}^h b \sigma_z z dz = 2b \int_0^h \sigma_z z dz \\ &= 2b \left[\int_0^{h'} \frac{\sigma_0}{h'} z^2 dz + \int_{h'}^h \frac{\sigma_0}{E_1 + F_2} \left(E_1 + F_2 \frac{z}{h'} \right) z dz \right] \\ &\quad \text{(from eqs. (2) and (7))} \\ &= \frac{b \sigma_0}{3(E_1 + F_2)} \cdot \frac{h^3}{h'} \left[2F_2 + 3E_1 \frac{h'}{h} - E_1 \left(\frac{h'}{h} \right)^3 \right] \end{aligned} \quad (8)$$

Hence,

$$\left(\frac{h'}{h} \right)^3 - 3 \left[1 - \left(1 + \frac{F_2}{E_1} \right) \frac{M}{b h^2 \sigma_0} \right] \left(\frac{h'}{h} \right) - 2 \frac{F_2}{E_1} = 0 \quad (9)$$

This equation shows how the thickness $2h'$ of layer in which the deformation is elastic, depends on the external moment M and time function $F_2(t)$. When the moment M is large, eq. (9) may approximate to

$$\frac{h}{h'} = \frac{3}{2} \left(1 + \frac{E_1}{F_2} \right) \frac{M}{bh^2\sigma_0} - \frac{E_1}{F_2} \quad (10)$$

because the thickness $2h'$ is small relative to the thickness $2h$ of beam and is reduced gradually with time after loading.

The deflection of beam v is determined by the differential equation

$$\frac{d^2v}{dx^2} = -\frac{\varepsilon_{h'}}{h'} = -\frac{\varepsilon_h}{h} \quad (11)$$

with the boundary conditions that

$$\left. \begin{aligned} v &= 0, & \text{at } x &= 0 \quad (\text{free support}) \\ \frac{dv}{dx} &= 0, & \text{at } x &= \frac{l}{2} \quad (\text{center of span}) \end{aligned} \right\} \quad (12)$$

From eqs. (6) and (10),

$$\frac{\varepsilon_{h'}}{h'} = \frac{\varepsilon_h}{h} = \frac{3\sigma_0}{2hE_1} \left[\left(1 + \frac{E_1}{F_2} \right) \frac{M}{bh^2\sigma_0} - \frac{E_1}{F_2} \right] \quad (13)$$

The solution of eq. (11) is

$$v = \frac{P(3l^2x - 4x^3)}{32bh^3E_1} + \left[\frac{P(3l^2x - 4x^3)}{32bh^3} - \frac{3\sigma_0(lx - x^2)}{4h} \right] \frac{1}{F_2} \quad (14)$$

($\because M = \frac{P}{2}x$)

The function $\frac{1}{F_2(t)}$ is approximated as follows,

$$\begin{aligned} \frac{1}{F_2(t)} &= \frac{1}{E_2} - \frac{2}{B_2E_2} \tanh^{-1} \left\{ \exp(-A_2B_2E_2t) \tanh \frac{B_2}{2} \right\} \\ &\simeq \frac{1}{E_2} - \frac{1}{B_2E_2} \log \frac{1 + (1 - A_2B_2E_2t) \tanh \frac{B_2}{2}}{1 - (1 - A_2B_2E_2t) \tanh \frac{B_2}{2}} \\ &\quad (\text{assumed } A_2B_2E_2t \ll 1) \\ &\simeq \frac{1}{E_2} - \frac{1}{B_2E_2} \log \frac{2 - A_2B_2E_2t}{A_2B_2E_2t} \\ &\quad (\text{assumed } \frac{B_2}{2} \gg 1) \\ &= \frac{1}{E_2} - \frac{1}{B_2E_2} \log \frac{2}{A_2B_2E_2t} \left(1 - \frac{A_2B_2E_2t}{2} \right) \\ &\simeq \frac{1}{E_2} + \frac{1}{B_2E_2} \log \frac{A_2B_2E_2t}{2} \end{aligned} \quad (15)$$

Therefore, eq. (14) is represented as

$$v = \frac{P(3l^2x - 4x^3)}{32bh^3E_1} + \left[\frac{P(3l^2x - 4x^3)}{32bh^3} - \frac{3\sigma_0(lx - x^2)}{4h} \right] \left[\frac{1}{E_2} + \frac{1}{B_2E_2} \log \frac{A_2B_2E_2t}{2} \right] \quad (16)$$

From this equation, it is inferred that the last term of deflection v is proportional to the logarithm of time and its proportional coefficient $g(x)$ is given by

$$g(x) = \frac{1}{B_2 E_2} \left[\frac{P(3l^2 x - 4x^3)}{32bh^3} - \frac{3\sigma_0(lx - x^2)}{4h} \right] \quad (17)$$

Noting g_1 and g_2 as $g(x)$ at $x = \frac{l}{2}$ and $x = \frac{l}{4}$ respectively,

$$\left. \begin{aligned} g_1 &= \frac{1}{B_2 E_2} \left[\frac{Pl^3}{32bh^3} - \frac{3l^2}{16h} \sigma_0 \right] \\ g_2 &= \frac{1}{B_2 E_2} \left[\frac{11}{16} \frac{Pl^3}{32bh^3} - \frac{3}{4} \frac{3l^2}{16h} \sigma_0 \right] \end{aligned} \right\} \quad (18)$$

and solving simultaneously these two equations for σ_0 and $B_2 E_2$, we have

$$\left. \begin{aligned} \sigma_0 &= \frac{1}{24} \frac{Pl}{bh^2} \frac{(11g_1 - 16g_2)}{(3g_1 - 4g_2)} \\ B_2 E_2 &= \frac{1}{128} \frac{Pl^3}{bh^3} \frac{1}{(3g_1 - 4g_2)} \end{aligned} \right\} \quad (19)$$

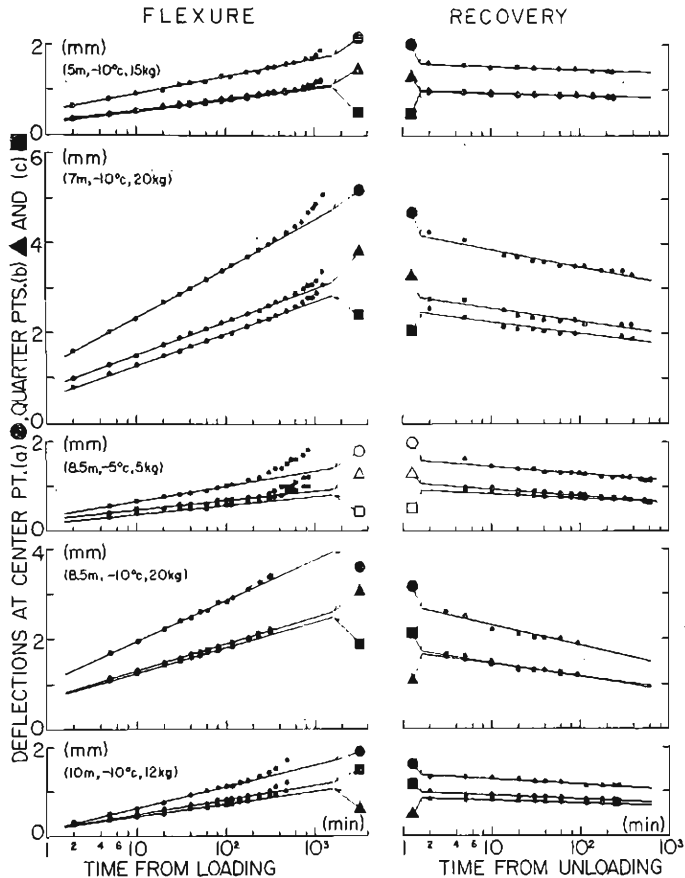


Fig. 5. Deflections and recoveries under various center load and temperature. Figures in parentheses represent sampling depth and center load weight.

5. Result of experiments and its consideration

The typical variation of deflection has already been shown in Figs. 2 and 3. Because eq. (16) is applied to the case of the stress σ smaller than the upper yield value σ_u , the results of deflection only where the beam was not broken was examined according to the method described in paragraph 4. Fig. 5 shows the plotted curves of v versus $\log t$ at various center loads. The deflections were increased linearly for several hundreds minutes after loading at -5°C and -10°C , and later along a curve concavely upward until unloading. Their recoveries were arranged on straight lines in all cases.

It was reported in Part I, that the compressive deformation in axial direction was analysed fairly well on semi-logarithmic graphs and the lower yield value σ_0 and important creep factor B_2E_2 of frozen soil were calculated from the experimental results, as shown in Table 3. It is interesting to consider whether those values were coincidental with the values calculated by eq. (19) from the results of deflections.

TABLE 3.

The values of creep factors σ_0 and B_2E_2 calculated from the results of axial contraction of frozen soil cylinder.

	Temperature of experiment ($^\circ\text{C}$)	Sampling depth (m)			
		5	7	8.5	10
σ_0 (kg/cm 2)	- 5	2.04	2.41	3.89	—
	-10	—	—	2.34	—
$B_2E_2 \times 10^{-4}$ (kg/cm 2)	- 5	2.28	1.78	6.39	—
	-10	—	—	6.86	—

Using the results of deflections of samples at the depths of 7, 8.5 and 10 m, the proportional coefficients g_1 and g_2 were determined by the least squares

TABLE 4.

The values of coefficients g_1 and g_2 determined by the least squares method, using the results of deflection of frozen soil beams.

Temperature of experiment ($^\circ\text{C}$)	Coeff. $g(x)$ of $\log_{10} t$	Sampling depth (m)			
		5	7	8.5	10
- 5	g_1 at pt. (a) (10^{-1}mm)	—	—	3.4	—
	g_2 at pt. (b) (, ,)	—	—	2.1	—
	g_2 at pt. (c) (, ,)	—	—	2.1	—
-10	g_1 at pt. (a) (10^{-1}mm)	3.8	11.1	9.1	4.9
	g_2 at pt. (b) (, ,)	2.6	7.2	5.7	3.2
	g_2 at pt. (c) (, ,)	2.6	7.5	5.7	2.5

TABLE 5.

The values of creep factors σ_0 and B_2E_2 calculated by eq. (19) from the results of deflection of frozen soil beam.

	Temperature of experiment (°C)	Sampling depth (m)			
		5	7	8.5	10
σ_0 (kg/cm ²)	- 5	—	—	1.4	—
	-10	0.4	2.9	5.1	2.4
$B_2E_2 \times 10^{-4}$ (kg/cm ²)	- 5	—	—	1.7	—
	-10	10.5	3.7	3.1	2.7

All figures in Table are the mean values of creep factors evaluated from the combinations the value of g_1 at center pt. (a) with the respective value of g_2 at quarter pt. (b) an (c).

method and the values of σ_0 and B_2E_2 were calculated. The results of calculation are shown in Tables 4 and 5.

It will be seen in Tables 3 and 5, that the values of σ_0 and B_2E_2 from the deflection were in fair agreement with those from the contraction.

However, the concaveness of deflection curve after several hundreds minutes from loading suggests that the beam might be broken if the period of loading was lengthened or that frozen soil beam might be deflected in a different manner from eq. (16) derived under assumptions described in paragraph 4. These questions will be considered in future.

6. Conclusion

An experiment of deflection of beam was carried out, using frozen soils sampled at an alluvial plane in Tokyo, and the important factors σ_0 and B_2E_2 of creep deformation were evaluated by analytical method of deflection, derived from certain assumptions. These values were compared with those calculated from the results of axial compression of the same frozen soil. The comparison showed fairly close agreement.

Acknowledgements

The writer wishes to express his sincere appreciation to Professors S. Okuda and S. Murayama of Kyoto University for their cordial guidance and encouragement in this work.

His thanks are also due to Dr. T. Takashi and T. Kato, members of the staff of the Seiken-Reiki Co., Ltd. for their valuable support.

References

- 1) Jackson, K. A., Uhlmann, D. R. and Chalmers, B., "Frost Heave in Soils", J. Appl. Phys., Vol. 37, No. 2 (1965), pp. 848-852.
- 2) Williams, P. J., "Unfrozen Water Content of Frozen Soils and Soil Moisture Suction", Geotechnique, Vol. 14, No. 3 (1964), pp. 231-246.
- 3) Jackson, K.A., Chalmers, B., "Freezing of Liquids in Porous Media with Special

- Reference to Frost Heave in Soils", J. Appl. Phys., Vol. 29, No. 8 (1958), pp. 1178-1181.
- 4) Uhlmann, D. R. and Chalmers, B., "Interaction, Between Particles and a Solid-Liquid Interface", J. Appl. Phys., Vol. 35, No. 10 (1964), pp. 2986-2993.
 - 5) Scheidegger, A. D., "Theoretical Geomorphology", Springer-Verlag, Berlin, 1961, pp. 45, 281-286.
 - 6) Jackson, K. A. and Uhlmann, D. R., "Particle Sorting and Stone Migration Due to Frost Heave", Science, Vol. 152, No. 3721 (1966), pp. 545-546.
 - 7) Takashi, T., Matsuura, I. and Taniguchi, H., "Dojo-Toketsu-Koho (The Freezing Method of Soil in Engineering Construction)", Reito (The Freezing), Vol. 36, No. 410, pp. 1082-1101, (In Japanese).
 - 8) Vialov, S. S., "Creep and Long-term Strength of Frozen Soils", Dok. Akad. Nauk SSSR, Vol. 104, No. 6 (1955), pp. 850-853.
 - 9) Fukuo Y., "On the Rheological Behavior of Frozen Soil (Part I)", Bull. Disaster Prevention Res. Inst., Kyoto Univ., Vol. 15, Part 3 (1966), pp. 1-7.
 - 10) Murayama, S. and Shibata, T., "On the Rheological Characters of Clay", Trans. of JSCE, No. 40, pp. 1-31.